Test of s-channel helicity conservation in inelastic ρ^0 diffraction in 20-GeV photoproduction

K. Abe,[m] T. C. Bacon,[e] J. Ballam,[k] A. V. Bevan,[e] H. H. Bingham,[o] J. E. Brau,[q] K. Braune,[k] D. Brick,[b] W. M. Bugg,[q] J. M. Butler,[k] W. Cameron,[e] H. O. Cohn,[i] G. Condo,[q] D. C. Colley,[a] S. Dado,[l] R. Diamond,[d] P. Dingus,[o] R. Erickson,[k] R. C. Field,[k] B. Franek,[j] N. Fujiwara,[h] R. Gearhart,[k] T. Glanzman,[k] I. M. Godfrey,[e] J. J. Goldberg,[l] A. T. Goshaw,[c] G. Hall,[e] E. R. Hancock,[j] T. Handler,[q] H. J. Hargis,[q] E. L. Hart,[q] M. J. Harwin,[e] K. Hasegawa,[m] R. I. Hulsizer,[g] M. Jobes,[a] G. E. Kalmus,[j] D. P. Kelsey,[j] T. Kitagaki,[m] A. Levy,[p] P. W. Lucas,[c] W. A. Mann,[n] E. McCrory,[c] R. Merenyi,[n] R. Milburn,[n] C. Milstene,[p] K. C. Moffeit,[k] A. Napier,[n] S. Noguchi,[h] F. Ochiai,[f] S. O'Neale,[a] A. P. T. Palounek,[c] I. A. Pless,[g] P. Rankin,[k] H. Sagawa,[m] T. Sato,[f] J. Schneps,[n] S. J. Sewell,[j] J. Shank,[o] A. M. Shapiro,[b] J. Shimony,[q] R. Sugahara,[f] A. Suzuki,[f] K. Takahashi,[f] K. Tamai,[m] S. Tanaka,[m] S. Tether,[g] D. A. Waide,[a] W. D. Walker,[c] M. Widgoff,[b] C. G. Wilkins,[a] S. Wolbers,[o] C. A. Woods,[j] A. Yamaguchi,[m] R. K. Yamamoto,[g] S. Yamashita,[h] Y. Yoshimura,[f] G. P. Yost,[o] and H. Yuta[m]

[a]*Birmingham University, Birmingham, B15 2TT, England*
[b]*Brown University, Providence, Rhode Island 02912*
[c]*Duke University, Durham, North Carolina 27706*
[d]*Florida State University, Tallahassee, Florida 32306*
[e]*Imperial College, London, SW7 2BZ, England*
[f]*National Laboratory for High Energy Physics (KEK), Oho-machi, Tsukuba-gun, Ibaraki 305, Japan*
[g]*Massachusetts Institute of Technology, Cambridge, Massachusetts 02139*
[h]*Nara Womens University, Kita-uoya, Nishi-Machi, Nara 630, Japan*
[i]*Oak Ridge National Laboratory, Oak Ridge, Tennessee 37830*
[j]*Rutherford Appleton Laboratory, Didcot, Oxon OX11 OOX, England*
[k]*Stanford Linear Accelerator Center, Stanford University, Stanford, California 94305*
[l]*Technion—Israel Institute of Technology, Haifa 32000, Israel*
[m]*Tohoku University, Sendai 980, Japan*
[n]*Tufts University, Medford, Massachusetts 02155*
[o]*University of California, Berkeley, California 94720*
[p]*University of Tel Aviv, Tel Aviv, Israel*
[q]*University of Tennessee, Knoxville, Tennessee 37996*
(SLAC Hybrid Facility Photon Collaboration)
(Received 25 March 1985)

The reaction $\gamma p \to \rho^0_{\text{fast}} p \pi^+ \pi^-$ has been studied with the linearly polarized 20-GeV monochromatic photon beam at the SLAC Hybrid Facility to test the prediction of s-channel helicity conservation in inelastic diffraction for $t' < 0.4$ (GeV/c)^2. In a sample of 1934 events from this reaction, the ρ^0 decay-angular distributions and spin-density-matrix elements are consistent with s-channel helicity conservation, the $\pi^+\pi^-$ mass shape displays the same skewing as seen in the reaction $\gamma p \to p\pi^+\pi^-$, and the $p\pi^+\pi^-$ mass distribution compares well and scales according to the vector dominance model with that produced in $\pi^\pm p \to \pi^\pm_{\text{fast}} p \pi^+ \pi^-$.

INTRODUCTION

Conservation of s-channel helicity (SCHC) in hadronic diffraction has been of experimental[1–8] and theoretical[9–11] interest for over a decade. SCHC follows naturally from QCD-based models of the Pomeron, such as two-gluon exchange.[12] Evidence for SCHC has been reported in the elastic-diffraction processes $\gamma p \to \rho p$ (Ref. 1) and $\pi N \to \pi N$ (Ref. 2). It has been speculated that it might also be valid in inelastic diffraction,[9] but this is not found to be true in πp (Ref. 3), Kp (Ref. 4), and pp (Refs. 5 and 10) experiments. Thus, SCHC is no longer viewed as a general rule for inelastic diffraction, although evidence suggests that in some cases the inelastic diffraction which displays nonconservation of s-channel helicity may result from two production mechanisms, one of which exhibits SCHC.[6,7] Furthermore, analysis based on the Deck model has explained the patterns of s- and t-channel helicity conservation in meson-diffraction dissociation.[11]

Polarized ρ mesons produced by linearly polarized photons on hydrogen provide a good test of SCHC. Previous work has shown evidence for SCHC in inclusive inelastic ρ^0 photoproduction.[8,13] If SCHC holds in the inelastic-diffractive reaction $\gamma p \to \rho N^*$, the polar- and azimuthal-

angular distributions of the ρ^0 decay in the helicity system will follow the well-known prediction[14]

$$W(\cos\theta,\Psi)=(3\sin^2\theta/8\pi)(1+P_\gamma\cos 2\Psi)$$

independent of t. In what follows we report evidence of SCHC in $\gamma p\to\rho N^*$ from an analysis of a clean sample of 1934 such events produced in the SLAC Hybrid Facility exposed to a linearly polarized 20-GeV photon beam.

EXPERIMENTAL DETAILS

The experiment has been described in previous publications.[15–18] The linearly polarized monochromatic photon beam is formed by backscattering an ultraviolet laser beam from the SLAC 30-GeV primary electron beam. The backscattered photons have a 52% linear polarization. The SLAC Hybrid Facility consists of a 40-in. hydrogen bubble chamber, with its flashlamps triggered by signals from downstream detectors: proportional wire chambers,[16] Cherenkov counters,[17] and a lead-glass wall.[18] The trigger accepts $(88\pm3)\%$ of the total cross section. The data presented here have been corrected on an event-by-event basis for the relatively small losses in the trigger efficiency. The average weight is 1.11 for the inelastic ρ^0 production events and the acceptance varies less than 20% over the t', mass, and angle ranges of the events used in the reaction $\gamma p\to\rho^0_{\text{fast}}p\pi^+\pi^-$.

EVIDENCE FOR DIFFRACTIVE INELASTIC ρ^0 PHOTOPRODUCTION

A sample of 6468 events having a three-constraint fit to the reaction $\gamma p\to p\pi^+\pi^+\pi^-\pi^-$ with total energy between 15 and 20 GeV has been selected from the 300 000 hadronic events measured in this experiment. Figure 1(a) shows the two-pion effective masses for this final state; histogram A is the spectrum for all $\pi^+\pi^-$ combinations (four per event), while curve B is the sum of spectra for the two same-sign combinations. The four-pion effective mass distribution, shown in Fig. 1(b), is dominated by $\rho'(1600)$ production. Figure 2 gives the two-pion momentum spectra for selections described below. From Figs. 1 and 2 the following qualitative conclusions can be drawn.

(a) The $\pi^+\pi^-$ mass spectrum [histogram A, Fig. 1(a)] shows a prominent ρ^0 signal which rises above the combinatorial background represented by histogram B.

(b) The $\rho'(1600)$ signal is enhanced if only those $\pi^+\pi^-$ masses in the ρ^0 region ($M_{\pi^+\pi^-}<1000$ MeV/c^2) are selected from histogram A in Fig. 1(a); this effect is demonstrated by histogram B in Fig. 1(b) and indicates that there is a substantial ρ^0 signal coming from the decay of $\rho'(1600)$.

(c) If the $\pi^+\pi^-$ system is further restricted to have momentum >16 GeV/c and $|t'|=|t-t_{\min}|<0.5$ (GeV/c)^2 the histogram C of Fig. 1(b) is obtained; the $\rho'(1600)$ signal is completely suppressed. This indicates that the ρ^0's coming from $\rho'(1600)$ decay have a much softer momentum spectrum than those produced diffractively.

(d) Curve A in Fig. 2 shows the momentum spectrum for $\pi^+\pi^-$ combinations having masses in the ρ^0 region

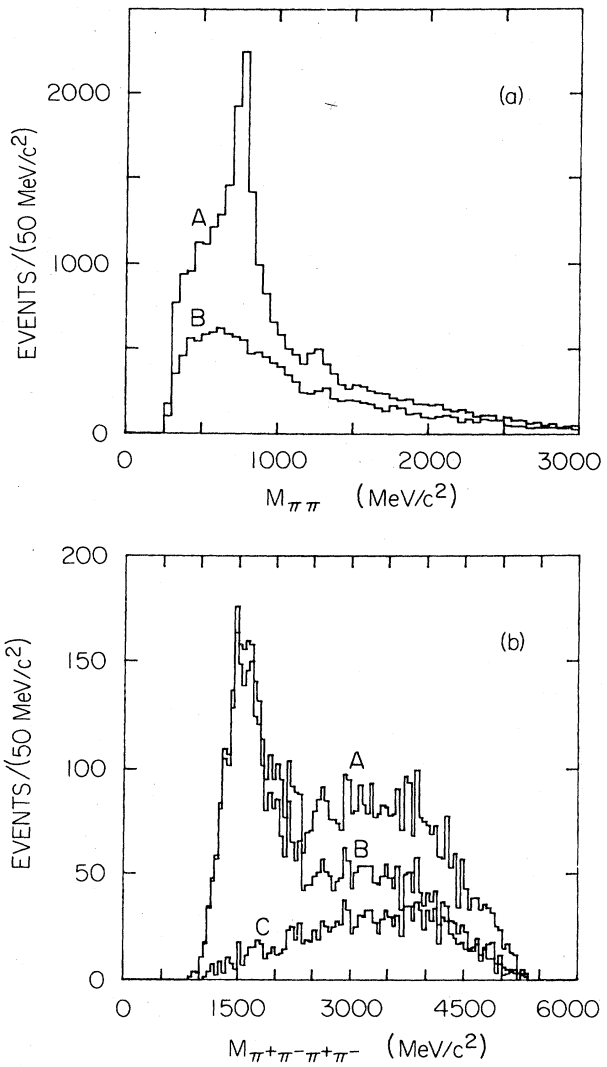

FIG. 1. (a) The $\pi\pi$ mass distributions for 6468 events of the reaction $\gamma p\to p\pi^+\pi^+\pi^-\pi^-$. A is $\pi^+\pi^-$ and B is $\pi^\pm\pi^\pm$. (b) The 4π mass distribution for the reaction. A is all 6468 events, B is the 4528 events with $M_{\pi^+\pi^-}<1000$ MeV/c^2 for at least one combination, and C is the 1614 events having one $\pi^+\pi^-$ combination with mass <1000 MeV/c^2, momentum >16 GeV/c, and $|t'_{\gamma\to\pi^+\pi^-}|<0.5$ (GeV/c)^2.

($M_{\pi^+\pi^-}<1000$ MeV/c^2) with $|t'|<1.0$ (GeV/c)^2. Only the largest momentum $\pi^+\pi^-$ pair in each event is included. There is a broad contribution centered at 10 GeV/c with a hard component beyond 16 GeV/c; this supports the conclusion, in (c) above, that the ρ^0's are produced both diffractively and in $\rho'(1600)$ decay. Those arising from $\rho'(1600)$ decay are shown by curve B where the mass of the four pions is less than 2400 MeV/c. An estimate from this distribution of the nondiffractive background above 16 GeV/c yields $(20\pm5)\%$.

(e) The momentum spectrum shape for ρ^0's produced elastically at the same incident gamma energy in the reaction $\gamma p\to p\pi^+\pi^-$ is shown in histogram C of Fig. 2 where there is a striking similarity with the hard com-

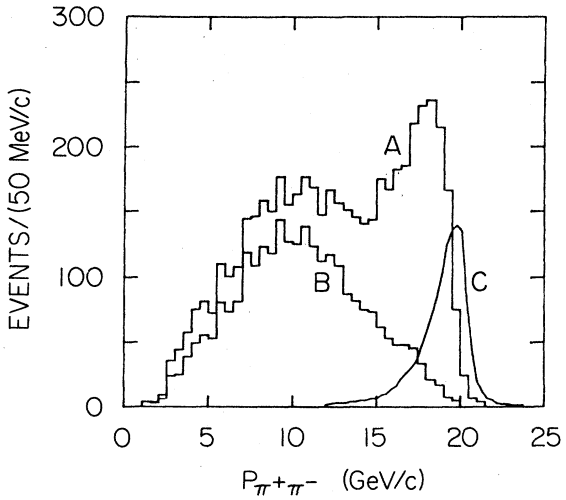

FIG. 2. The $\pi^+\pi^-$ momentum spectrum for $M_{\pi^+\pi^-} < 1000$ MeV/c^2. A is for the largest momentum $\pi^+\pi^-$ with $|t'| < 1.0$ (GeV/c)^2 (5102 events), B is for those which also have $M_{4\pi} < 2400$ MeV/c^2 (2643 events), and C is the $\pi^+\pi^-$ momentum spectrum from the reaction $\gamma p \to p\rho^0$ ($\rho^0 \to \pi^+\pi^-$) plotted to an arbitrary scale.

ponent of histogram A, although histogram A is shifted to lower momenta by the more restrictive phase space resulting from the massive recoiling baryon system.

(f) Finally, selecting only those events containing $\pi^+\pi^-$ pairs having momentum greater than 16 GeV/c gives the mass spectrum shown in Fig. 3(a) which is clearly dominated by ρ^0 production and displays the mass-skewing exhibited in the quasielastic reaction $\gamma p \to \rho^0 p$ shown in Fig. 3(b).

This selection of events with $\pi^+\pi^-$ pairs having a momentum in excess of 16 GeV/c produces a sample of diffractively produced ρ^0's from the reaction $\gamma p \to p\pi^+\pi^-\pi^+\pi^-$, which is free from $\rho'(1600)$ feedthrough. The $\pi^+\pi^-$ mass distribution has been fitted by a curve representing the Söding model[19] of the form

$$\frac{d\sigma}{dm} = (f_{\rho D} + f_{\rho ND})\sigma_\rho(m) + f_I I(m) + f_D D(m) + f_B B(m) .$$

The four terms which contribute to this expression have the following origin:

(a) The Breit-Wigner term representing ρ production, both diffractive and nondiffractive:

$$\sigma_\rho(m) = \frac{m}{q} \frac{m_\rho \Gamma_\rho(m)}{(m_\rho^2 - m^2)^2 + m_\rho^2 \Gamma_\rho^2(m)} .$$

(b) The Drell amplitude, which represents the nonresonant $\pi^+\pi^-$ production from the photon:

$$D(m) = \frac{(m^2 - m_\rho^2)^2}{(m_\rho^2 - m^2)^2 + m_\rho^2 \Gamma_\rho^2(m)} .$$

(c) A term representing the interference of the diffractive ρ amplitude with the Drell amplitude:

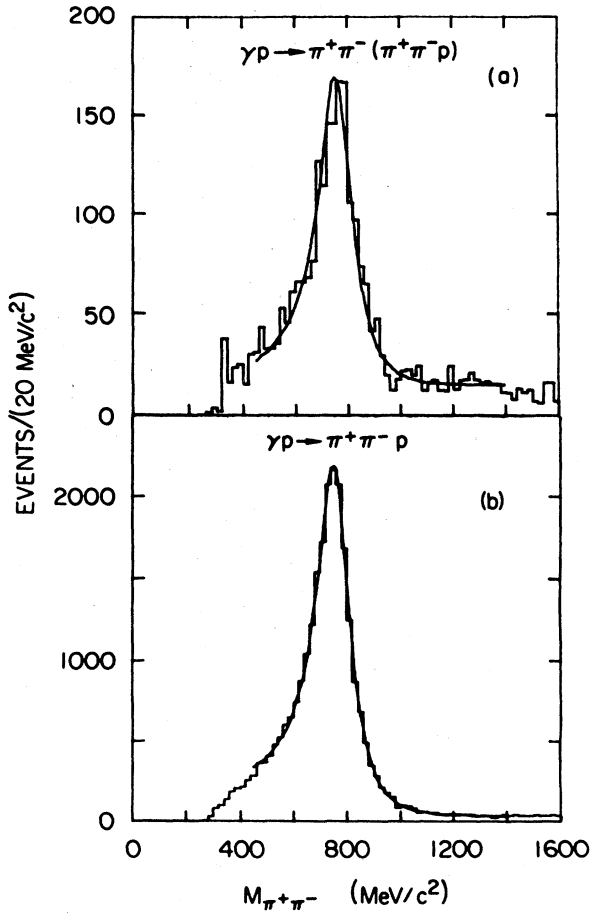

FIG. 3. (a) The $\pi^+\pi^-$ mass distribution for the fast pairs selected as described in the text (2580 events, 2890 after weights). The fit is to the Söding model (see text). (b) Söding-model fit to the $\pi^+\pi^-$ distribution for the reaction $\gamma p \to p\rho^0$ at 20 GeV/c.

$$I(m) = \frac{m^2 - m_\rho^2}{(m_\rho^2 - m^2)^2 + m_\rho^2 \Gamma_\rho^2(m)} .$$

(d) A polynomial nonresonant background:

$$B(m) = (m - 2m_\pi) + b(m - 2m_\pi)^2 + c(m - 2m_\pi)^3 ,$$

where b and c are parameters of the fit.

The parameters $f_{\rho D}$, $f_{\rho ND}$, f_D, f_I, and f_B represent the strengths of the following terms: the diffractive ρ^0, the nondiffractive ρ^0, the Drell mechanism, the Drell-ρ interference, and the nonresonant background. A fit to the quasielastic distribution shown in Fig. 3(b) was done with $f_{\rho ND}$ and f_B set to zero. The relative strengths of f_D, f_I, and $f_{\rho D}$ were then fixed in the inelastic fit. The integrated contribution from $f_{\rho ND}$ and f_B below 1000 MeV/c^2 was constrained to 20% as suggested earlier from Fig. 2. In the above,

$$\Gamma_\rho(m) = \Gamma_0 [q(m)/q(m_\rho)]^3 \frac{\rho(m)}{\rho(m_\rho)} ,$$

$$\rho(m) = [q^2(m) + q^2(m_\rho)]^{-1} ,$$

where q is the pion momentum in the center of mass of the dipion system and m_ρ and Γ_0 are the ρ^0 mass and width (769±3 MeV/c^2 and 154±5 MeV/c^2, respectively). The ρ^0 mass and width were allowed to vary in the final fit, the effects of which were included in the χ^2 with the above cited errors.

The Breit-Wigner term is symmetric around the position of the ρ mass; asymmetry about the ρ pole is produced by the interference term. Skewness in the mass spectrum is therefore evidence for a departure from pure ρ production. Fractions of each process present have been fitted to the mass spectrum using a minimum χ^2 method; the full form shown above gives a χ^2 of 75 for 42 degrees of freedom compared to a value of 1088 if only the Breit-Wigner term is allowed to contribute.

In order to isolate the reaction $\gamma p \to \rho^0(p\pi^+\pi^-)$ we select only those events from Fig. 3 with $M_{\pi\pi} < 1000$ MeV/c^2. Figure 4(a) shows the $p\pi^+\pi^-$ mass distribution for the pions opposite the selected $\pi\pi$ systems and compares this distribution with that of the diffractive reaction[20] $\pi^\pm p \to \pi^\pm(p\pi^+\pi^-)$ at 14 GeV/c. If we are indeed observing a diffractive reaction we would expect to be able to relate it to the pion-induced diffraction through the equation

$$\sigma_{\gamma p \to \rho N^*} = \frac{\alpha}{2}\left[\frac{f_\rho{}^2}{4\pi}\right]^{-1}(\sigma_{\pi^+ p \to \pi^+ N^*} + \sigma_{\pi^- p \to \pi^- N^*}),$$

where $f_\rho{}^2/4\pi = 2.18$, determined by comparing quasielastic $\gamma p \to \rho^0 p$ to elastic $\pi^\pm p$ scattering.[21] Figure 4(a) shows a comparison of our data with such a renormalization of the π-induced diffraction. The agreement is very good in the relevant region ($M_{p\pi^+\pi^-} < 2000$ MeV/c^2). Both distributions show similar features, with the photoproduction being about 10% less. The diffractive nature is further supported by observing the near equality of our measured cross section of 0.90±0.1 μb with the value reported[22] for $\gamma p \to \rho^0 \Delta^{++}\pi^-$ at 9.3 GeV of 1.0±0.3 μb. Figure 4(b) shows the $p\pi^+$ mass distribution from the $p\pi^+\pi^-$ system. The $p\pi^+\pi^-$ system is clearly dominated by $\Delta^{++}\pi^-$. We have also observed a small component of $\Delta^0\pi^+$, consistent with the expected $\frac{1}{9}$ contribution for the decay of an N^* with isotopic spin $\frac{1}{2}$. The t' distribution for the reaction has a slope which depends on the mass of the $p\pi^+\pi^-$ system as shown in Table I, with the largest slopes occurring for the smaller masses. This is the same dependence as in π-induced diffraction and similar to the variation observed with $\pi\pi$ mass in elastic $\pi\pi$ photoproduction.

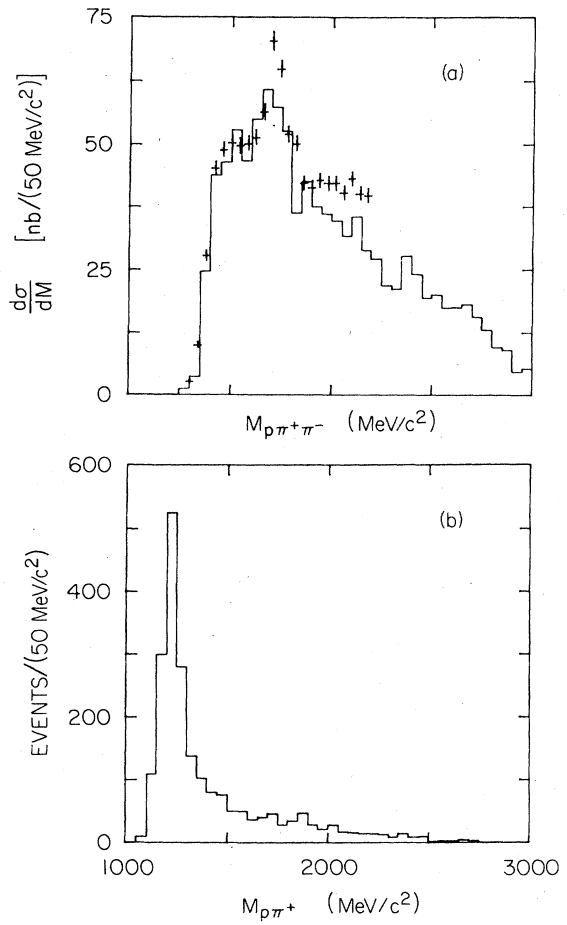

FIG. 4. (a) The $p\pi^+\pi^-$ mass distribution for the 1934 events (2144 after weights) with fast $\pi^+\pi^-$ pairs of mass <1000 MeV/c^2. The data points are from the reaction (Ref. 20) $\pi^\pm p \to \pi^\pm_{\text{fast}}(p\pi^+\pi^-)$ where the total number of events with $M_{p\pi^+\pi^-} < 2200$ MeV/c^2 has been renormalized by a vector-dominance-model factor (see text). (b) The $p\pi^+$ mass distribution for the events in (a).

TABLE I. The slope b of the differential cross section ($dN/dt' = A\,e^{bt'}$) as a function of the ($p\pi^+\pi^-$) mass [for the four-momentum transfer squared from the photon to the $\rho^0(t' = t - t_{\min})$] for $|t'| < 0.4$ (GeV/c)^2.

$M_{p\pi^+\pi^-}$ (MeV/c^2)	b [(GeV/c)$^{-2}$]
<1500	8.75±0.49
1500–1600	10.66±0.60
1600–1800	5.08±0.30
1800–2100	5.53±0.31
>2100	3.21±0.23

Finally, we have observed diffractive inelastic ρ^0 production as evidenced by the peripheral nature, the ρ-mass skewing, the similarity and scaling of the $p\pi^+\pi^-$ mass distribution to π-induced diffraction, and the isotopic spin-$\frac{1}{2}$ behavior of the $\Delta\pi$ branching ratios.

THE TEST OF s-CHANNEL HELICITY CONSERVATION

To test SCHC of the ρ^0 we have examined the distributions of conventional helicity angles.[23] Figure 5 illustrates these angles. The polar angle of the π^+ in the ρ-rest frame relative to the ρ direction of flight is denoted by θ. The difference between the azimuthal angles (Φ, the angle between the photon polarization vector and the production plane in the center-of-mass system, and ϕ, the azimuthal angle of the ρ decay in the ρ-rest frame measured as the angle between the decay plane and the production plane) is denoted by Ψ ($\Psi = \phi - \Phi$). If s-channel helicity

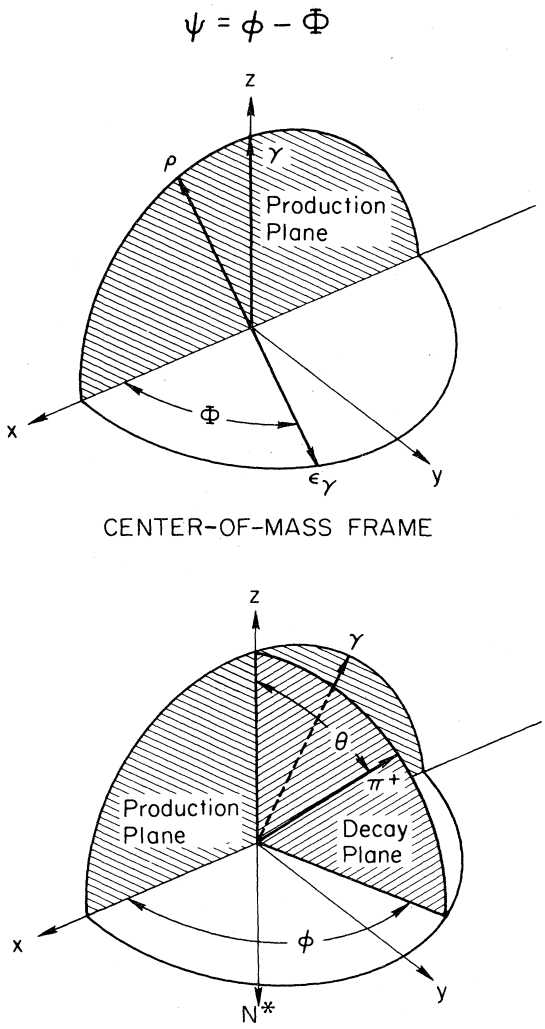

FIG. 5. The angles used in the study of ρ^0 decay. The y axis is the normal to the production plane, defined by the cross product $\hat{\mathbf{k}}\times\hat{\mathbf{p}}$ of the directions of the photon and the vector meson. The x axis is given by $\hat{\mathbf{x}}=\hat{\mathbf{y}}\times\hat{\mathbf{z}}$.

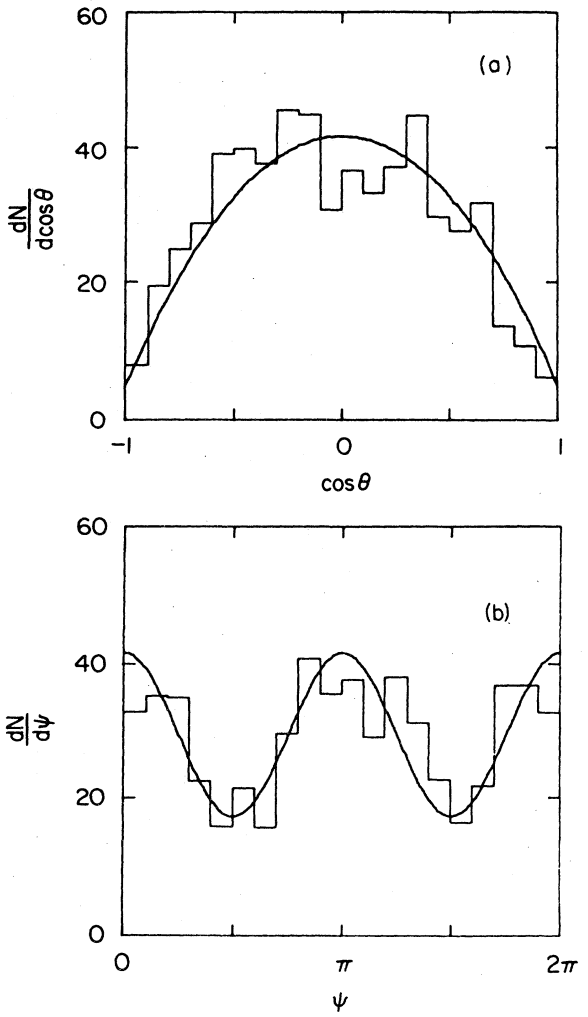

FIG. 6. The decay-angular distributions of the $\pi^+\pi^-$ system in the helicity frame for the mass range 720 MeV/c^2 $<M_{\pi^+\pi^-}<$ 820 MeV/c^2. The data represent 532 events (588 after weights) and the superimposed curves are the expected distribution for SCHC including a 20% background (with an isotropic angular distribution) and a photon polarization of 52%.

is conserved the ρ will have helicity ±1 and

$$W(\cos\theta,\Psi)=\left[\frac{3}{8\pi}\sin^2\theta\right](1+P_\gamma\cos2\Psi)\ .$$

$P_\gamma=0.52$ is the calculated degree of photon polarization, verified by the elastic ρ measurements.[24]

Figure 6 presents the distributions for $\cos\theta$ and Ψ for this reaction[25] with the further restriction, $720<M_{\pi\pi}<820$ MeV/c^2 (along with the previous cuts $P_{\pi^+\pi^-}>16$ GeV/c, $M_{p\pi^+\pi^-}<2200$ MeV/c^2). The solid curves give the prediction of SCHC and include a contribution from 20% background which is assumed to be isotropic, $W(\cos\theta,\Psi)=1/4\pi$. This angular distribution for the background was found to be consistent with that of the $\pi^+\pi^-$ pairs in the region $P_{\pi^+\pi^-}\sim10$ GeV/c. There is good agreement with the expected SCHC behavior indicating that this reaction is dominated by SCHC.

To assess quantitatively the degree of s-channel helicity conservation for inelastic ρ^0 production, the density matrix elements of the ρ^0 decay in the helicity rest frame have been determined. The decay angular distribution can be expressed in terms of nine independent measurable spin-density-matrix elements ρ^α_{ik}

$$\begin{aligned}W(\cos\theta,\phi,\Phi)=\frac{3}{4\pi}[\ &\tfrac{1}{2}(1-\rho^0_{00})+\tfrac{1}{2}(3\rho^0_{00}-1)\cos^2\theta-\sqrt{2}\,\mathrm{Re}\rho^0_{10}\sin2\theta\cos\phi-\rho^0_{1-1}\sin^2\theta\cos2\phi\\&-P_\gamma\cos2\Phi(\rho^1_{11}\sin^2\theta+\rho^1_{00}\cos^2\theta-\sqrt{2}\,\mathrm{Re}\rho^1_{10}\sin2\theta\cos\phi-\rho^1_{1-1}\sin^2\theta\cos2\phi)\\&-P_\gamma\sin2\Phi(\sqrt{2}\,\mathrm{Im}\rho^2_{10}\sin2\theta\sin\phi+\mathrm{Im}\rho^2_{1-1}\sin^2\theta\sin2\phi)]\ .\end{aligned}$$

TABLE II. The spin-density-matrix elements for the diffractive ρ^0 meson in the helicity reference frame. These matrix elements have been corrected for the (20±5)% nondiffractive background in the final data sample. This background is assumed to have an isotropic angular distribution.

	$0.0<\lvert t'\rvert<0.4$ (GeV/c)^2	$0.4<\lvert t'\rvert<1.0$ (GeV/c)^2
ρ^0_{00}	−0.01±0.02	−0.01±0.03
$\mathrm{Re}\rho^0_{10}$	0.03±0.02	−0.01±0.05
ρ^0_{1-1}	−0.02±0.03	−0.02±0.06
ρ^1_{11}	0.05±0.08	0.14±0.19
ρ^1_{00}	0.04±0.11	0.38±0.18
$\mathrm{Re}\rho^1_{10}$	0.10±0.08	−0.10±0.15
ρ^1_{1-1}	0.28±0.11	0.61±0.24
$\mathrm{Im}\rho^2_{10}$	−0.05±0.07	0.37±0.17
$\mathrm{Im}\rho^2_{1-1}$	−0.39±0.12	−0.69±0.24

For transverse and linearly polarized photons, one expects, in the case of SCHC, that only two spin-density-matrix elements are nonzero

$$\rho^1_{1-1}=\tfrac{1}{2} \quad \text{and} \quad \mathrm{Im}\rho^2_{1-1}=-\tfrac{1}{2} .$$

The values for two t' bins are shown in Table II; these are from the angular distributions after removal of the 20% isotropic background. In general, the helicity flip density matrices remain small as t' increases, e.g., $\rho^0_{00}\sim 0$ for all t', and the nonflip terms are consistent with their expected values.

CONCLUSION

In conclusion, we find that the features of ρ^0 decay in inelastic diffraction $\gamma p\to\rho N^*$ are consistent with s-channel helicity conservation as determined from the decay angular distributions and the spin-density matrix elements. Furthermore, the inelastically produced ρ^0 displays the same mass skewing as the elastically produced ρ^0. The nucleon dissociation mass spectrum is similar to that found in pion-induced nucleon diffraction dissociation and its cross section is similar to that calculated from the vector dominance model.

ACKNOWLEDGMENTS

We wish to thank the SLAC bubble-chamber crew for their dedication to this experiment and the film scanners and measurers at the many institutions for their careful processing of the events. We especially thank Joe Murray for his work on the beam. We have benefited from discussion of the theory of this reaction with F. J. Gilman. The work was supported by the Japan-U.S. Cooperative Research Project on High Energy Physics under the Japanese Ministry of Education, Science, and Culture, the U.S. Department of Energy, the Science and Engineering Research Council (United Kingdom), the U.S. National Science Foundation, and the U.S.-Israel Academy of Sciences Commission for Basic Research.

[1]J. Ballam *et al.*, Phys. Rev. Lett. **24**, 960 (1970).
[2]F. Halzen and C. Michael, Phys. Lett. **36B**, 367 (1971); A. Delesquez *et al.*, *ibid.* **40B**, 77 (1972); G. Gozzika *et al.*, *ibid.* **40B**, 281 (1972); V. Barger and F. Halzen, Phys. Rev. Lett. **28**, 194 (1972).
[3]Yu. M. Antipov *et al.*, Nucl. Phys. **B63**, 153 (1973).
[4]F. Grard *et al.*, Lett. Nuovo Cimento **2**, 305 (1971); J. V. Beaupré *et al.*, Phys. Lett. **34B**, 160 (1971); B. Buschbeck *et al.*, Nucl. Phys. **B35**, 511 (1971); J. V. Beaupré *et al.*, *ibid.* **B47**, 51 (1972); G. W. Brandenburg *et al.*, *ibid.* **B45**, 397 (1972); R. Barloutaud *et al.*, *ibid.* **B59**, 374 (1972).
[5]N. G. Albrow *et al.*, Nucl. Phys. **B108**, 1 (1976).
[6]G. Berlad *et al.*, Nucl. Phys. **B78**, 29 (1974).
[7]P. Bosetti *et al.*, Nucl. Phys. **B101**, 304 (1975).
[8]E. Kogan *et al.*, Nucl. Phys. **B122**, 383 (1977).
[9]F. Gilman, J. Pumplin, A. Schwimmer, and L. Stodolsky, Phys. Lett. **31B**, 387 (1970).
[10]J. Pumplin, Phys. Scr. **25**, 191 (1981).
[11]E. L. Berger and J. T. Donohue, Phys. Rev. D **15**, 790 (1977).
[12]J. Randa, in *Proceedings of the XIth International Winter Meeting on Fundamental Physics, Toledo, Spain, 1983,* edited by A. Ferrando (Instituto de Estudies Nucleares, Madrid, 1983).
[13]K. C. Moffeit *et al.*, Phys. Rev. D **5**, 1603 (1972).
[14]G. Wolf, Nucl. Phys. **B26**, 317 (1971).
[15]K. Abe *et al.*, Phys. Rev. D **30**, 1 (1984).
[16]R. C. Field *et al.*, Nucl. Instrum. Methods **200**, 237 (1982).
[17]A. Bevan *et al.*, Nucl. Instrum. Methods **203**, 159 (1982).
[18]J. E. Brau *et al.*, Nucl. Instrum. Methods **196**, 403 (1983).
[19]D. Aston *et al.*, Nucl. Phys. **B209**, 56 (1982); P. Söding, Phys. Lett. **19**, 702 (1966).
[20]G. B. Chadwick *et al.*, Phys. Rev. D **17**, 1713 (1978).
[21]For a review, see T. H. Bauer, R. D. Spital, D. R. Yennie, and F. M. Pipkin, Rev. Mod. Phys. **50**, 261 (1978).
[22]H. H. Bingham *et al.*, Phys. Lett. **41B**, 635 (1972).
[23]K. Schilling, P. Seyboth, and G. Wolf, Nucl. Phys. **B15**, 397 (1970); **B18**, 332(E) (1970).
[24]K. Abe *et al.*, Phys. Rev. Lett. **53**, 751 (1984).
[25]Twenty-two percent of the experiment was excluded from the angular distribution analysis (as in Ref. 24) since the ultraviolet laser photons had a deteriorated polarization.